journal

J. Am. Ceram. Soc., **86** [8] 1256–61 (2003)

Paralinear Oxidation of Silicon Nitride in a Water-Vapor/Oxygen Environment

Dennis S. Fox,* Elizabeth J. Opila,*,† QuynhGiao N. Nguyen,* Donald L. Humphrey,‡ and Susan M. Lewton§

John H. Glenn Research Center at Lewis Field, National Aeronautics and Space Administration, Cleveland, Ohio 44135

Three Si_3N_4 materials were exposed to dry oxygen flowing at 0.44 cm/s at temperatures between 1200° and 1400°C. Weight change was measured using a continuously recording microbalance. Parabolic kinetics were observed. When the same materials were exposed to a 50% H_2O–50% O_2 gas mixture flowing at 4.4 cm/s, all three types exhibited paralinear kinetics. The material was oxidized by water vapor to form solid SiO_2. The protective SiO_2 was in turn volatilized by water vapor to form primarily gaseous $Si(OH)_4$. Nonlinear least-squares analysis and a paralinear kinetic model were used to determine parabolic and linear rate constants from the kinetic data. Volatilization of the protective SiO_2 scale could result in accelerated consumption of Si_3N_4. Recession rates under conditions more representative of actual combustors were compared with the furnace data.

I. Introduction

THE high strength, high temperature capability, and low density of silicon-based ceramics, such as silicon nitride (Si_3N_4) and silicon carbide (SiC), make them candidate materials for application in the hostile environments of advanced aeropropulsion engines. The dry oxidation behavior of Si_3N_4 has been studied in great detail.[1–6] If silicon-based ceramics are to be used in combustion applications, their behavior under fuel-lean conditions must be determined. Jacobson[1] has calculated equilibrium products resulting from fuel-lean combustion of Jet A aviation fuel ($CH_{1.9185}$). The products include O_2, H_2O, CO_2, and N_2. Independent of the fuel-to-air ratio, the amount of water vapor remains almost constant at ~10%. In such an environment, the primary oxidant is water vapor:[7]

$$Si_3N_4(s) + 6H_2O(g) = 3SiO_2(s) + 2N_2(g) + 6H_2(g) \quad (1)$$

Others have recognized the need to study the oxidation of Si_3N_4 in water-vapor-containing environments.[8–14] However, none have measured kinetics continuously. In general, it has been found that, above a few volume percent water vapor, the oxidation rate of Si_3N_4 increases with water-vapor content. This also has been shown for SiC.[15] It has been demonstrated for SiC that, in addition to the oxidation reaction, water vapor simultaneously reacts with the growing SiO_2 scale to form a volatile species.[16–18] This species has been identified as $Si(OH)_4(g)$,[19] which forms by the following reaction:

$$SiO_2(s) + 2H_2O(g) = Si(OH)_4(g) \quad (2)$$

The simultaneously occurring oxidation and volatilization reactions have been modeled using paralinear kinetics.[16,20] The kinetics can be described by

$$t = \frac{\alpha^2 k_p}{2(k_l^2)}\left[\frac{-2k_l\Delta w_1}{\alpha k_p} - \ln\left(1 - \frac{2k_l\Delta w_1}{\alpha k_p}\right)\right] \quad (3)$$

$$\Delta w_2 = -\beta k_l t \quad (4)$$

For Si_3N_4, $\alpha = MW_{SiO_2}/(MW_{O_2} - \frac{2}{3}MW_{N_2})$ and $\beta = MW_{SiN_{1.3}}/MW_{SiO_2}$, where MW is the molecular weight, k_p the oxidation parabolic rate constant in units of specific weight squared versus time ($mg^2/(cm^4 \cdot h)$), k_l the linear rate constant ($mg/(cm^2 \cdot h)$), Δw_1 the weight gain from SiO_2 growth, Δw_2 the weight loss from SiO_2 volatilization, and t the oxidation time.

The objective of this paper is to determine the oxidation behavior of three Si_3N_4 materials in dry oxygen and in 50% H_2O–50% O_2 from 1200° to 1400°C. Nonlinear least-squares analysis and a paralinear kinetic model described in Ref. 16 are used to determine k_p and k_l from the continuously measured weight change data during the water-vapor exposures. Recession of the substrate under the furnace conditions is estimated. Si_3N_4 recession rates from the furnace data are extrapolated to more realistic, high-velocity conditions. These are compared with experimental results from a high-pressure burner rig that operates at conditions more typical of combustion applications.

II. Experimental Procedure

The materials used in this study are described in Table I. The α-Si_3N_4 is produced via chemical vapor deposition (Advanced Ceramics Corp., Cleveland, OH). SN282 (Kyocera Industrial Ceramics Corp., Vancouver, WA) is a high-strength β-Si_3N_4 with an improved oxidation-resistant grain-boundary phase developed for gas-turbine applications. The AS800 material (AlliedSignal Ceramic Components, Torrance, CA) is an *in situ*-reinforced β-Si_3N_4 developed to enable a new generation of power systems. A rare-earth-based sintering system is used in production of the material, resulting in an apatite grain-boundary phase.

Specimens were cleaned using a detergent solution, distilled water, acetone, and alcohol. Specimen weight was measured on an analytical pan balance (±0.01 mg) before exposure and at the end of the experiment. Oxidation experiments were conducted in a vertical-tube furnace at three temperatures: 1200°, 1300°, and 1400°C (all ±10°C). Fused-quartz furnace tubes were used (Quartz Scientific, Fairport Harbor, OH). The oxidation kinetics were followed using thermogravimetric analysis (TGA). Weight change was continuously monitored using a recording microbalance (Model C-1000, Cahn Instruments, Cerritos, CA). Specimens were suspended on sapphire hangers inside a 2.5 cm ID vertical

D. Butt—contributing editor

Manuscript No. 187109. Received March 13, 2002; approved April 3, 2003.

*Member, American Ceramic Society.
†Cleveland State University Resident Research Associate at NASA GRC.
‡QSS Group, Inc., Brookpark, OH; Research Technician at NASA GRC.
§Work performed while a NASA/Ohio Aerospace Institute summer intern; currently at Department of Chemical Engineering, Purdue University, West Lafayette, IN.

Table I. Silicon Nitride Materials

	CVD Si_3N_4	SN282 Si_3N_4	AS800 Si_3N_4
Manufacturer	Advanced Ceramics Corporation	Kyocera Industrial Ceramics Corporation	AlliedSignal Ceramic Components
Major additives/impurities[†]			
Major	None	Lu	La, Y, Sr
Minor	C, O	W, C	C
ppm	H, Al, Fe	Yb, Ca, Mg, Y, Fe, Ba, Mn, Sr	Ba, Fe
Density (g/cm^3)	3.18	3.37	3.32
TGA sample size (cm)	2.5 × 0.7 × 0.3	2.6 × 1.3 × 0.3	2.5 × 1.3 × 0.3
Surface area (cm^2)	7.8	9.1	9.0

[†]Major is >1%, Minor is 0.1–1.0%.

furnace tube. Initial experiments were conducted with dry oxygen flowing at 0.44 cm/s in a fused-quartz tube. Because of the high sensitivity of the microbalance used to measure very small weight changes, the flow rate was kept low to minimize noise in the kinetic curve.

For the subsequent water-vapor–oxygen tests, an experimental apparatus based on a design by Belton and Richardson[21] was used. A schematic is found in Ref. 15. The reaction gas was introduced at the bottom of the fused-quartz furnace tube. Water was added to the oxygen by first over-saturating the gas with deionized water. A high flow rate of 4.4 cm/s was needed to enable saturation of the gas stream. The gas then passed through a glass-bead-filled saturator immersed in a water bath held at 81.7°C. The resulting oxygen stream was saturated with 50% water vapor. A counterflow of oxygen through the top of the TGA apparatus was used to keep water from condensing on the microbalance and hang wire. At least two specimens of each Si_3N_4 material were run at each of the three test temperatures. Weight change versus time was continuously measured during the 100 h. In this experiment, deposition of volatile products on the hang down occurred.[16] Control experiments were conducted with the sapphire hanger alone, and a linear weight gain was measured because of SiO_2 volatilization from the quartz tube and subsequent deposition on the hang down. This gain was subtracted from the weight data acquired for each Si_3N_4 sample.

To compare TGA furnace recession rates with those measured under conditions more representative of actual combustors, CVD and AS800 Si_3N_4 were also exposed in the NASA GRC high-pressure burner rig (HPBR) under fuel-lean conditions.[17] Additional HPBR tests of SN282 Si_3N_4 have been conducted. The rig itself is described in detail in Ref. 18. Weight change and sample thickness measurements were made every 8–16 h. The linear rate constants were obtained from the kinetic data, as were the parabolic rate constants when available.

The surface oxide was characterized using X-ray diffractometry (XRD) following TGA exposure of the as-received specimens. Oxide morphologies were then studied using scanning electron microscopy (SEM; Model JSM-840A, JEOL, Tokyo, Japan). Polished cross sections of selected samples were prepared to measure the SiO_2 scale thickness. One of the ~2.5 cm × 0.3 cm edges was polished to a 15 μm finish for observation using SEM and entailed oxide thickness measurements every 1 mm along the 25 mm edge. The average thickness for each selected specimen has been reported. A National Institute of Standards and Technology calibration standard was used to establish the appropriate correction factor for reporting thickness. It was determined that the measured thickness was ~5.3% greater than the true thickness.

III. Results

(1) Dry Oxygen

Each of the three Si_3N_4 materials exhibits parabolic behavior in dry oxygen. The average parabolic rate constants in this environment are listed in Table II with the calculated activation energies for the oxide formation. Parabolic rate constants for each sample as a function of reciprocal temperature are shown in Fig. 1. The pure CVD Si_3N_4 is the most oxidation-resistant material. The Lu-containing SN282 Si_3N_4 is more oxidation resistant than the La-containing AS800 Si_3N_4.

After TGA exposure, the surface oxide (Fig. 2) is characterized using XRD. The oxide grown on CVD Si_3N_4 at 1200°C is amorphous, with α-cristobalite observed after 1300° and 1400°C exposures. After exposure of the Lu-containing SN282 Si_3N_4, α-cristobalite and $Lu_2Si_2O_7$ are observed. Lu_2SiO_5 is also present at $T \geq 1300$°C. The AS800 oxide is α-cristobalite, with Y_2O_3 also present only at 1400°C. The cracks in the surface oxide are formed from the β- to α-cristobalite transformation on cooling.

(2) 50% H_2O–50% O_2

In 50% H_2O–50% O_2 flowing at 4.4 cm/s, paralinear kinetics are observed for all three Si_3N_4 materials (Fig. 3). Although CVD Si_3N_4 initially gains weight in the water-vapor environment, a change to a linear weight loss occurs after ~20 h. This is due to the volatilization of the SiO_2 scale that occurs concurrently with the oxidation. The noise in the curves is due to the high sensitivity of the microbalance scale required to measure the very small weight changes (~0.1 mg/cm^2) and to the high 4.4 cm/s flow rate.

Once the paralinear nature of the reaction in 50% H_2O–50% O_2 is established, the parabolic oxidation rate constants (k_p) and the linear volatility rate constants (k_l) can be determined. The fit of the model to the data is shown as the solid line in Fig. 3. This is the sum of the weight changes from the oxidation and volatilization reactions, as determined using the nonlinear least-squares analysis of the data. Table III summarizes the parabolic and linear rate

Table II. Average Parabolic Rate Constants (k_p) of Si_3N_4 Determined from TGA Experiments in Dry Oxygen

	k_p ($mg^2/(cm^4 \cdot h)$)		
	CVD Si_3N_4	SN282 Si_3N_4	AS800 Si_3N_4
Temperature (°C)			
1200	$5.6\ (\pm 1.3) \times 10^{-6}$	$1.8\ (\pm 0.9) \times 10^{-5}$	$2.1\ (\pm 0.2) \times 10^{-4}$
1300	$1.6\ (\pm 0.6) \times 10^{-5}$	$5.5\ (\pm 1.4) \times 10^{-5}$	$3.4\ (\pm 0.3) \times 10^{-4}$
1400	$5.2\ (\pm 0.8) \times 10^{-5}$	$1.2\ (\pm 0.4) \times 10^{-4}$	$8.0\ (\pm 1.6) \times 10^{-4}$
Activation energy (kJ/mol)	227 ± 44	204 ± 79	135 ± 31

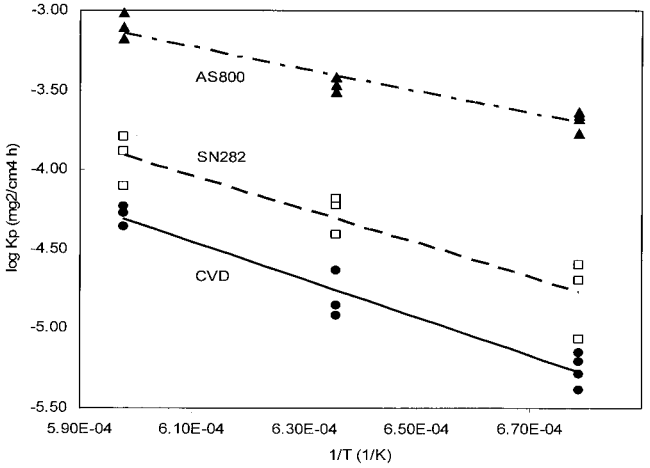

Fig. 1. Parabolic rate constants (k_p) for the three Si_3N_4 materials in dry oxygen flowing at 0.44 cm/s

constants for the three Si_3N_4 materials from the paralinear data in 50% H_2O–50% O_2.

The volatility fluxes determined experimentally for the three Si_3N_4 materials are plotted in an Arrhenius diagram in Fig. 4. The activation energy (E_a) from a fit of all the data points (solid line) is calculated to be 36 ± 86 kJ/mol (95% confidence interval), which indicates little temperature dependence. Representative photographs after 1400°C exposures are shown in Fig. 5. Oxide thickness measurements, for single specimens after exposure in 50% H_2O–50% O_2, are listed in Table IV. The oxides grown on CVD Si_3N_4 at 1200° and 1300°C are too thin to measure using this technique, as is that on SN282 Si_3N_4 at 1200°C.

XRD of CVD Si_3N_4 at 1200°C shows the oxide to be amorphous. α-cristobalite is observed after 1300° and 1400°C exposures. In comparison, Choi *et al.*,[13] observed amorphous SiO_2 after steam exposure of CVD Si_3N_4 at 1000°–1300°C for 10 h. In the present study, after exposure of the Lu-containing SN282 Si_3N_4, α-cristobalite and $Lu_2Si_2O_7$ are observed using XRD. The AS800 oxides are identified as α-cristobalite, Y_2O_3, and $La_2Si_2O_7$.

(3) High-Pressure Burner Rig

The only material to exhibit paralinear behavior in the HPBR was AS800 Si_3N_4. Table V summarizes the parabolic and linear rate constants for AS800 Si_3N_4 determined from the paralinear data. The measured k_p in the 0.6 atm P_{H_2O} burner rig of $\sim 5 \times 10^{-2}$ $mg^2/(cm^4 \cdot h)$ is higher than the $\sim 1 \times 10^{-3}$ $mg^2/(cm^4 \cdot h)$ measured in the 0.5 atm P_{H_2O} TGA (1 atm = 1×10^5 Pa). Impurities within the burner rig are thought to enhance oxidation. The CVD Si_3N_4 and SN282 Si_3N_4 materials exhibit linear weight loss. A weight-loss rate comparison under standard fuel-lean conditions in the HPBR is shown in Fig. 6. As in the TGA experiments, SN282 Si_3N_4 exhibits the lowest recession rates. This is likely due to formation of $Lu_2Si_2O_7$ in the surface oxide, which results in a decrease of SiO_2 volatility.

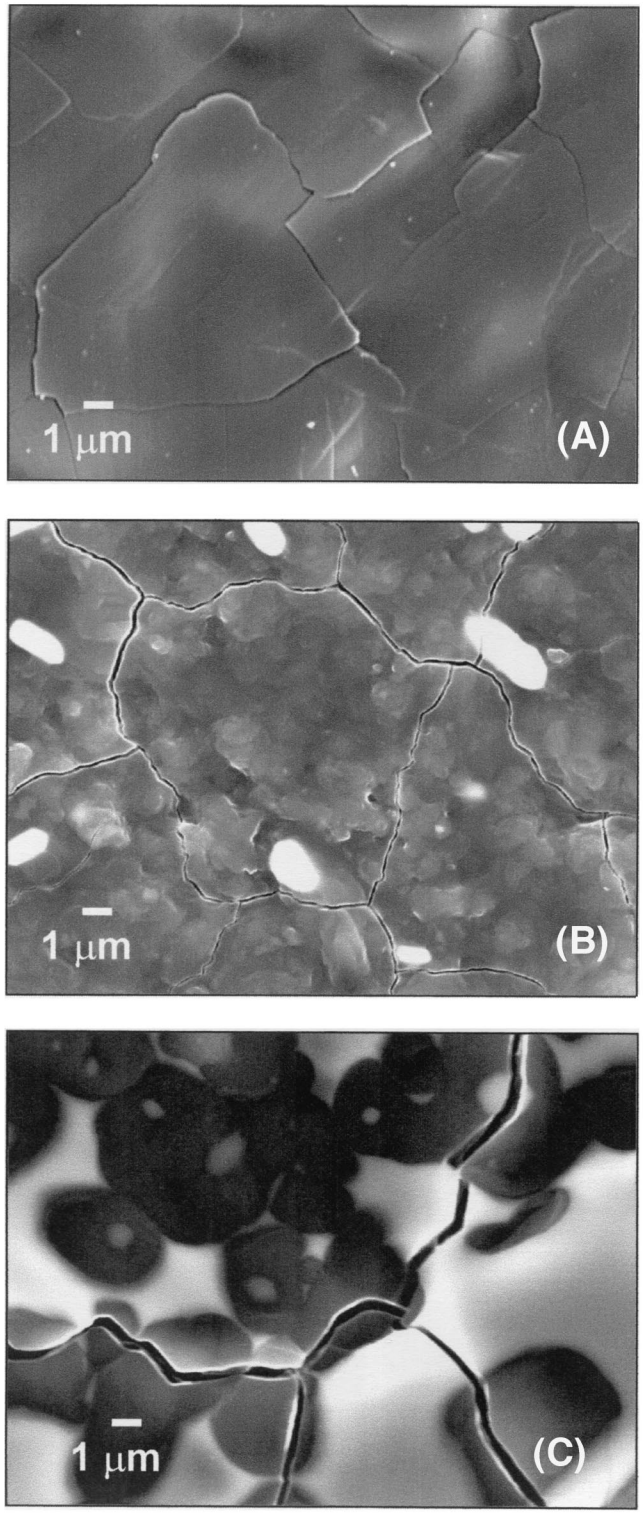

Fig. 2. Surface morphology of Si_3N_4 after 100 h at 1400°C in dry oxygen: (A) CVD; (B) SN282; and (C) AS800.

IV. Discussion

(1) Parabolic Behavior in Dry Oxygen

The CVD Si_3N_4 is the most oxidation-resistant material (Fig. 1) because of the formation of an oxynitride phase between the SiO_2 and substrate.[2–3] The mechanism is different in additive-containing materials. In their study of the oxidation of hot-pressed Si_3N_4 containing either MgO[4] or Y_2O_3,[5] Cubicciotti and Lau have deduced that the rate-limiting step is the diffusion of additive cations through the grain boundary to the surface oxide. $MgSiO_3$ and $Y_2Si_2O_7$ are observed in the cristobalite surface oxide. Measured activation energies are 440 and 450 kJ/mol, respectively. Clarke[6] believes the growth of pure SiO_2 creates a gradient with the additive-containing silicate grain-boundary phase, driving the cations to the surface oxide.

The SN282 Si_3N_4 oxidation mechanism is not clear. $Lu_2Si_2O_7$ is present in the surface oxide of the SN282 Si_3N_4 material. However, the 204 kJ/mol activation energy is lower than Cubicciotti and Lau's findings and higher than Deal and Grove's 119 kJ/mol for single-crystal silicon. Others have studied the oxidation of Si_3N_4 containing lanthanide rare-earth elements (which can also include yttrium and scandium).[22–24] There is no clear correlation between the type of additive and oxidation resistance. Oxidation is

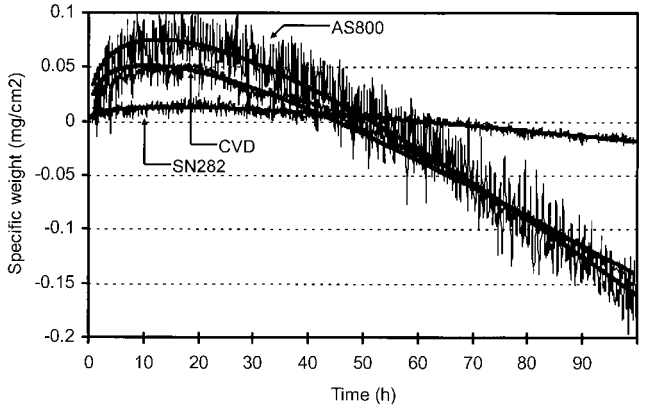

Fig. 3. Paralinear weight change kinetics for CVD, SN282, and AS800 Si_3N_4 at 1200°C in 50% H_2O–50% O_2 flowing at 4.4 cm/s. Solid line is the result of the least-squares analysis of the data.

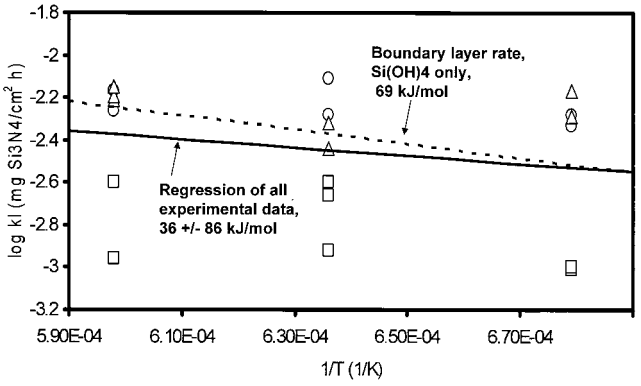

Fig. 4. Linear rate constants (k_l) for all Si_3N_4 materials in 50% H_2O–50% O_2 flowing at 4.4 cm/s ((△) CVD, (□) SN282, and (○) AS800).

complicated in that it is a function of cation movement and the nature of the grain-boundary phase. The La-containing AS800 Si_3N_4 is less oxidation resistant than SN282 Si_3N_4. The as-received AS800 Si_3N_4 has various grain-boundary phases—apatite and oxynitride. The oxide scale formed at 1200°C is solid and uniform. At higher temperatures, the scale morphology is rough, with glasslike nodules visible. The emergence of liquid phases allows much more rapid oxygen ingress.

(2) Paralinear Behavior in 50% Water Vapor

The paralinear nature of the reaction kinetics of Si_3N_4 with 50% H_2O–50% O_2 is obvious from the kinetic curves. Additional evidence is provided by comparison of calculated weight change, from SEM oxide measurements, with that actually measured. For oxidation alone, the oxide thickness (x) and weight gain (in mg/cm^2) are related by the expression

$$x = 19.4\Delta wt \tag{5}$$

when cristobalite is formed.[25] Assuming no volatility and using the measured oxide thickness, one calculates positive weight gains for each of the materials (Table IV). However, there is a clear discrepancy when the samples are weighed on the analytical pan balance. Actual weight gains are much less than that calculated, and, in two cases, overall weight losses are observed. The AS800 Si_3N_4 sample at 1400°C does not follow this trend because of formation of a low-viscosity scale. It is therefore evident that, although an oxide is continually being formed, volatilization of the SiO_2 by H_2O is also occurring. The ultimate result of this paralinear behavior is recession of the underlying Si_3N_4 substrate and subsequent weight loss.

The k_l values measured for CVD Si_3N_4, AS800 Si_3N_4, SiO_2,[16] and CVD SiC[16] under the same conditions are comparable. The k_l values for SN282 Si_3N_4 are slightly lower than those for the other materials. This may be attributed to the formation of $Lu_2Si_2O_7$ in the oxide, resulting in a lower silicon activity. When the Table III k_l data are plotted on an Arrhenius diagram (Fig. 4), only slight temperature dependence across the range of 1200°–1400°C is observed for all three Si_3N_4 materials.

The measured k_p values in 50% H_2O–50% O_2 in this study (Table III) are 1–2 orders of magnitude higher than those measured in dry oxygen (Table II), as is expected for SiO_2 formers. Water vapor enhances the oxidation rate in SiC[26] and silicon.[27] Very small weight gains are measured early in the experiment and occur at the ragged edge of the microbalance's sensitivity. The k_p is determined from a curve fit to the data, leading to scatter in the results and large standard deviations in the rate constants and activation energies.

The k_l values are the more essential parameters derived from the paralinear modeling. The recession calculations described below are based on the SiO_2 volatilization kinetics.

(3) Linear Weight-Loss Rates

The measured flux (Table III) can be compared with the calculated flux.[28] The appropriate relation for the flux of the volatile species from a flat plate through a gaseous boundary layer under laminar flow conditions is[29]

$$J = 0.664\left(\frac{\rho' vL}{\eta}\right)^{1/2}\left(\frac{\eta}{\rho' D}\right)^{1/3}\frac{D\rho}{L} \tag{6}$$

where J is the flux, ρ' the concentration of the major gas species, v the linear gas velocity, L the sample length, η the gas viscosity, D the interdiffusion coefficient for the diffusing species in the major gas species, and ρ the concentration of the diffusing gas species at the solid–gas interface. Gas concentration is calculated using the ideal gas law. Hashimoto[30] has measured thermodynamic data for $Si(OH)_4$. Krikorian[31] and Allendorf *et al.*[32] have calculated data for the Si-O-H system. Using these data in a free-energy minimization code (CHEMSAGE, GTT Technologies, Sweden), one can calculate vapor pressures of Si-O-H species. For

Table III. Average Parabolic (k_p in mg/(cm^2·h)) and Linear (k_l in mg/(cm^2·h)) Rate Constants of Si_3N_4 Determined from TGA Experiments in 50% H_2O–50% O_2

	CVD Si_3N_4		SN282 Si_3N_4		AS800 Si_3N_4	
	k_p	k_l	k_p	k_l	k_p	k_l
Temperature (°C)						
1200	8.8 ($\pm$1.0) $\times 10^{-4}$	5.0 ($\pm$0.4) $\times 10^{-3}$	9.3 ($\pm$6.7) $\times 10^{-5}$	9.8 ($\pm$0.1) $\times 10^{-4}$	1.7 ($\pm$0.1) $\times 10^{-3}$	5.9 ($\pm$1.1) $\times 10^{-3}$
1300	3.5 ($\pm$2.4) $\times 10^{-4}$	6.5 ($\pm$1.7) $\times 10^{-3}$	4.2 ($\pm$2.5) $\times 10^{-4}$	2.0 ($\pm$0.7) $\times 10^{-3}$	8.6 ($\pm$1.8) $\times 10^{-4}$	4.2 ($\pm$0.9) $\times 10^{-3}$
1400	1.0 ($\pm$0.1) $\times 10^{-3}$	6.2 ($\pm$0.9) $\times 10^{-3}$	4.5 ($\pm$2.2) $\times 10^{-4}$	1.8 ($\pm$1.0) $\times 10^{-3}$	5.2 ($\pm$0.9) $\times 10^{-2}$	6.6 ($\pm$0.5) $\times 10^{-3}$
Activation energy (kJ/mol)	20 $\pm$ 211	22 $\pm$ 51	174 $\pm$ 200	55 $\pm$ 111	338 $\pm$ 413	14 $\pm$ 60

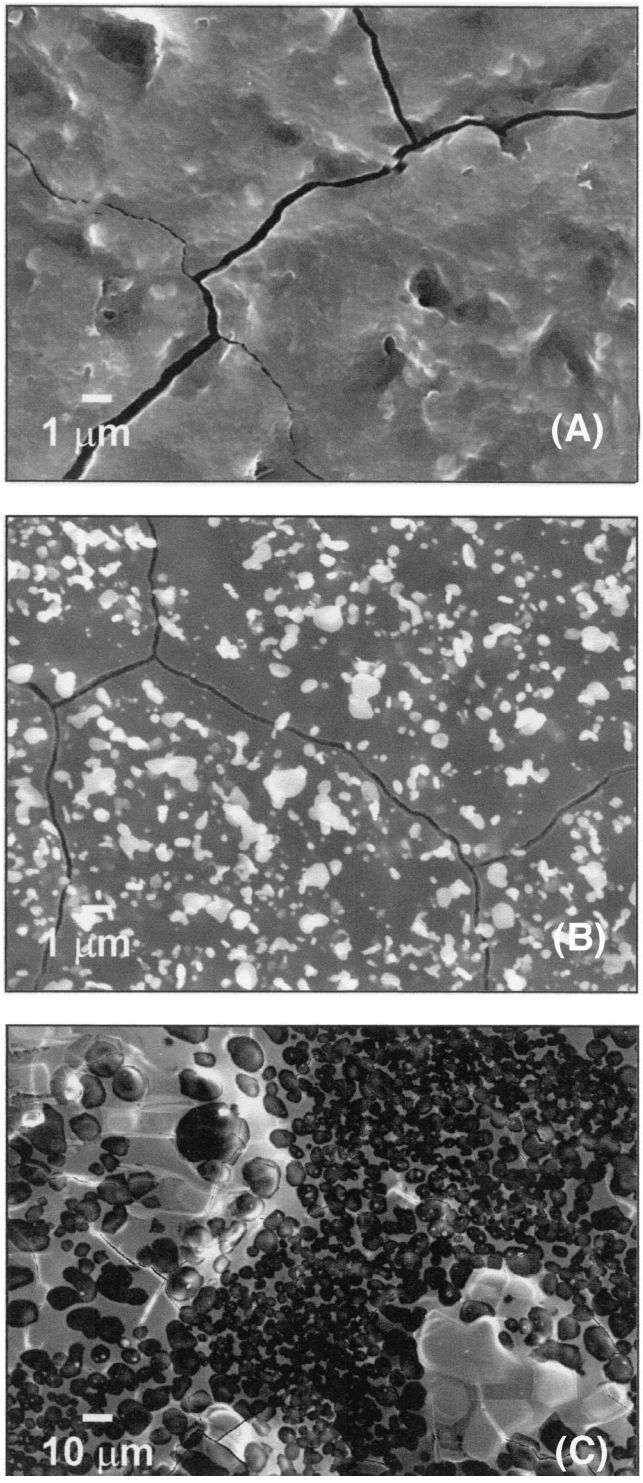

Fig. 5. Surface morphology of Si_3N_4 after 100 h at 1400°C in 50% H_2O–50% O_2: (A) CVD; (B) SN282; and (C) AS800.

these calculations, SiO_2 (cristobalite) plus an initial gas composition of 50% H_2O–50% O_2 has been used. The calculated vapor pressures of Si-O-H species are then used in the boundary layer diffusion model, and Si_3N_4 mass loss rates are determined. The best agreement with the experimental data ($E_a = 36 \pm 86$ kJ/mol) is for $Si(OH)_4$ as the primary volatile species ($E_a = 69$ kJ/mol). This calculated mass loss rate is shown in Fig. 4 as the dotted line. $SiO(OH)_2$ formation does not correlate with the experimental data, because the calculated mass loss rates are ~10 times larger[31] or ~10 times smaller[32] than those measured experimentally, and the activation energy is high at 205 kJ/mol. Thus the *magnitude* and temperature dependence of the measured flux is best described by $Si(OH)_4$ formation.

(4) Material Recession and Life Prediction

Many combustion applications require components to be used for thousands of hours. If the component is fashioned from Si_3N_4 and is operating in a fuel-lean environment, some concerns need to be addressed. The linear rate constant given in terms of weight loss can be directly related to recession of the substrate. After an initial period, the rate of SiO_2 volatilization is equivalent to the rate at which SiO_2 is formed. Because at long times the *substrate* is consumed to form the SiO_2 at the same rate that the SiO_2 is being volatilized, *substrate recession* can be estimated using k_l. A target recession limit used by this laboratory for combustor liner applications is 2.5×10^{-6} cm/h (10 mil/10 000 h (1 mil = 10^{-3} in.)). For CVD Si_3N_4 with a density of 3.2 g/cm^3, this equates to a maximum allowable k_l of 8×10^{-3} mg/(cm^2·h). The values listed in Table III are slightly lower than this allowable limit.

The TGA experiments provide an acceptable simulation of the temperature and water-vapor partial pressures found in an engine environment. However, engines operate at high total pressures. The flow rates encountered in a turbine engine are also much higher than the 4.4 cm/s used in the TGA experiments. At higher flow rates and system pressures, flux estimates can be made using a simplified form of Eq. (6). For this approximation, the diffusion coefficient (D) is proportional to $1/P_{total}$, and ρ' is proportional to P_{total}. Assuming that $Si(OH)_4(g)$ is the only volatile species and is formed via the reaction in Eq. (2), then ρ is proportional to $P_{Si(OH)_4}$:

$$k_l \propto \frac{v^{1/2} P_{H_2O}^2}{P_{total}^{1/2}} \tag{7}$$

For example, under the combustion conditions of 1200°C (2200°F), gas velocity (v) of 21 m/s (63 ft/s), P_{total} of 600 kPa (6 atm), and $P_{H_2}O$ of 60 kPa (0.6 atm), the calculated k_l is ~13 times the furnace k_l. Using AS800 Si_3N_4 as an example (3.32 g/cm^3), with its average k_l of 5.9×10^{-3} mg/(cm^2·h) from the 1200°C furnace data, the material's recession rate would be 2.28×10^{-5} cm/h (91 mil/10 000 h). This is an order of magnitude higher than the acceptable limit. This increase is due to much higher combustion gas velocity ($v^{1/2}$ component in Eq. (7)).

The conditions described in the preceding paragraph are those *actually used* for the high-pressure burner rig testing of all three silicon nitrides under fuel-lean conditions. For an AS800 Si_3N_4 specimen exposed at 1232°C, the measured k_l is 7.5×10^{-2} mg/(cm^2·h) (Table V). This correlates to a recession rate of 2.26×10^{-5} cm/h (89 mil/10 000 h)—virtually the same rate predicted above from the furnace results at 1200°C.

Si_3N_4 linear weight loss and surface recession result from SiO_2 scale volatility as shown in the TGA experiments as well as in more realistic burner rig tests. A considerable amount of substrate recession can occur after only hundreds of hours of exposure in the latter. Those proposing to use Si_3N_4 components in a fuel-lean combustion application, such as a turbine engine, must therefore be aware that SiO_2 volatility can occur and result in loss of component cross-sectional area.

V. Summary and Conclusions

Si_3N_4 exhibits parabolic kinetics when exposed to a dry-oxygen environment flowing at 0.4 cm/s in a fused-quartz furnace tube at 1200°–1400°C. However, the material exhibits paralinear kinetics when exposed in a 50 H_2O–50% O_2 gas mixture flowing at 4.4 cm/s. The material is oxidized by water vapor to form solid SiO_2. The protective SiO_2, in turn, is volatilized by water vapor to form primarily gaseous $Si(OH)_4$. At long exposure times, the kinetics can be approximated using the linear rate constants from the volatilization reaction. As a result of this exposure, accelerated consumption of Si_3N_4 occurs.

Table IV. Comparison of Calculated Weight Change from SEM Cross-Section Measurements with Actual Measured Weight in 50% H_2O–50% O_2 Flowing at 4.4 cm/s

Si_3N_4 material	Exposure temperature (°C)	Time (h)	SEM oxide thickness (μm)	Calculated Δ*wt* (mg/cm^2) from oxide thickness	Measured Δ*wt* (mg/cm^2) from pan balance
CVD	1400	100	3.88 ± 0.88	0.200	−0.274
SN282	1300	98	1.81 ± 0.29	0.093	+0.029
SN282	1400	100	5.51 ± 1.09	0.284	+0.009
AS800	1200	100	2.99 ± 0.96	0.154	−0.152
AS800	1300	98	5.33 ± 1.89	0.274	+0.006
AS800	1400	98	9.96 ± 2.97	0.513	+0.716

Table V. Parabolic and Linear Rate Constants of AS800 Si_3N_4 Determined from HPBR Experiments

Temperature (°C)	k_p (mg^2/(cm^4·h))	k_l (mg/(cm^2·h))
1163	5.0×10^{-2}	5.7×10^{-2}
1168	7.0×10^{-2}	5.7×10^{-2}
1232	5.1×10^{-2}	7.5×10^{-2}
1296	4.8×10^{-2}	1.0×10^{-1}

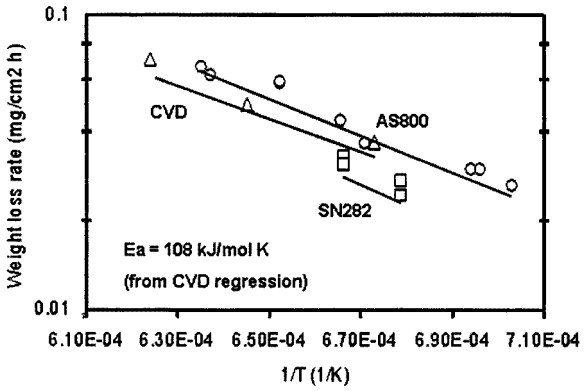

Fig. 6. Comparison of Si_3N_4 weight loss in the GRC high-pressure burner rig under standard fuel-lean conditions (sample temperature of 1150°–1330°C, gas velocity of 21 m/s, and total pressure of 600 kPa).

Recession rates determined from the furnace experiments can be used to estimate substrate recession under more realistic combustion conditions. Component recession, predicted from TGA results and observed under fuel-lean combustion conditions ($T = 1200$°C, $P = 6$ atm, $v_{gas} = 20$ m/s), is on the order of 2.5×10^{-5} cm/h (1 mil/100 h). Engine designers must be aware of the possible rapid recession of Si_3N_4 under turbine engine combustion conditions. Performance of turbine vanes or blades, with their thin trailing edges, are especially at risk from this mechanism of degradation.

Acknowledgment

The authors would like to offer their sincere thanks to Ralph G. Garlick and Dereck F. Johnson of the NASA Glenn Research Center at Lewis Field for the X-ray diffraction results and chemical analysis of the starting materials, respectively.

References

[1]N. S. Jacobson, "Corrosion of Silicon-Based Ceramics in Combustion Environments," *J. Am. Ceram. Soc.*, **76** [1] 3–28 (1993).

[2]H. Du, R. E. Tressler, K. E. Spear, and C. G. Pantano, "Oxidation Studies of Crystalline CVD Silicon Nitride," *J. Electrochem. Soc.*, **136** [5] 1527–36 (1989).

[3]L. U. J. T. Ogbuji and E. J. Opila, "A Comparison of the Oxidation Kinetics of SiC and Si_3N_4," *J. Electrochem. Soc.*, **142** [3] 925–30 (1995).

[4]D. Cubicciotti and K. H. Lau, "Kinetics of Oxidation of Hot-Pressed Silicon Nitride Containing Magnesia," *J. Am. Ceram. Soc.*, **61** [11–12] 512–17 (1978).

[5]D. Cubicciotti and K. H. Lau, "Kinetics of Oxidation of Yttria Hot-Pressed Silicon Nitride," *J. Electrochem. Soc.*, **126** [10] 1723–28 (1979).

[6]D. R. Clarke, "Thermodynamic Mechanism for Cation Diffusion through an Intergranular Phase: Applications to Environmental Reactions with Nitrogen Ceramics"; pp. 421–26 in *Progress in Nitrogen Ceramics*, NATO ASI Series, Series E: Applied Sciences, No. 65. Edited by F. L. Riley. Martinus Nijhoff, The Hague, The Netherlands, 1983.

[7]E. J. Opila and Q. N. Nguyen, "The Oxidation of CVD Silicon Carbide in Carbon Dioxide," *J. Am. Ceram. Soc.*, **81** [7] 1949–52 (1998).

[8]S. C. Singhal, "Effect of Water Vapor on the Oxidation of Hot-Pressed Silicon Nitride and Silicon Carbide," *J. Am. Ceram. Soc.*, **59** [1–2] 81–82 (1976).

[9]M. I. Mayer and F. L. Riley, "Sodium-Assisted Oxidation of Reaction-Bonded Silicon Nitride," *J. Mater. Sci.*, **13**, 1319–28 (1978).

[10]T. Sato, K. Haryu, T. Endo, and M. Shimada, "High-Temperature Oxidation of Silicon Nitride-Based Ceramics by Water Vapour," *J. Mater. Sci.*, **22**, 2635–40 (1987).

[11]M. Maeda, K. Nakamura, and T. Ohkubo, "Oxidation of Silicon Nitride in a Wet Atmosphere," *J. Mater. Sci.*, **24**, 2120–26 (1989).

[12]M. Maeda, K. Nakamura, and M. Yamada, "Oxidation Resistance of Silicon Nitride Ceramics with Various Additives," *J. Mater. Sci.*, **25**, 3790–94 (1990).

[13]D. J. Choi, D. B. Fishbach, and W. D. Scott, "Oxidation of Chemically-Vapor-Deposited Silicon Nitride and Single-Crystal Silicon," *J. Am. Ceram. Soc.*, **72** [7] 1118–23 (1989).

[14]E. Proverbio, D. Rossi, and R. Cigna, "Influence of Water Vapour on High-Temperature Oxidation of Al_2O_3–MgO-Doped Hot-Pressed Silicon Nitride," *J. Eur. Ceram. Soc.*, **9**, 453–58 (1992).

[15]E. J. Opila, "Oxidation Kinetics of Chemically Vapor-Deposited Silicon Carbide in Wet Oxygen," *J. Am. Ceram. Soc.*, **77** [3] 730–36 (1994).

[16]E. J. Opila and R. E. Hann, "Paralinear Oxidation of CVD SiC in Water Vapor," *J. Am. Ceram. Soc.*, **80** [1] 197–205 (1997).

[17]J. L. Smialek, R. C. Robinson, E. J. Opila, D. S. Fox, and N. S. Jacobson, "SiC and Si_3N_4 Recession Due to SiO_2 Scale Volatility Under Combustor Conditions," *Adv. Compos. Mater.*, **8** [1] 33–45 (1999).

[18]R. C. Robinson and J. L. Smialek, "SiC Recession Caused by SiO_2 Scale Volatility under Combustion Conditions: I, Experimental Results and Empirical Model," *J. Am. Ceram. Soc.*, **82** [7] 1817–25 (1999).

[19]E. J. Opila, D. S. Fox, and N. S. Jacobson, "Mass Spectrometric Identification of $Si(OH)_4$ from the Reaction of Silica with Water Vapor," *J. Am. Ceram. Soc.*, **80** [4] 1009–12 (1997).

[20]C. S. Tedmon Jr., "The Effect of Oxide Volatilization on the Oxidation Kinetics of Cr and Fe–Cr Alloys," *J. Electrochem. Soc.*, **113** [8] 766–68 (1967).

[21]G. R. Belton and F. D. Richardson, "A Volatile Iron Hydroxide," *Trans. Faraday Soc.*, **50**, 1562–72 (1962).

[22]D. M. Mieskowski and W. A. Sanders, "Oxidation of Silicon Nitride Sintered with Rare-Earth Oxide Additions," *J. Am. Ceram. Soc.*, **68** [7] C-160–C-163 (1985).

[23]M. K. Cinibulk and G. Thomas, "Oxidation Behavior of Rare-Earth Disilicate–Silicon Nitride Ceramics," *J. Am. Ceram. Soc.*, **75** [8] 2044–49 (1992).

[24]H.-J. Choi, J.-G. Lee, and Y.-W. Kim, "Oxidation Behavior of Hot-Pressed Si_3N_4 with Re_2O_3 (Re = Y, Yb, Er, La)," *J. Eur. Ceram. Soc.*, **19**, 2757–62 (1999).

[25]D. S. Fox, "Oxidation Behavior of Chemically-Vapor-Deposited Silicon Carbide and Silicon Nitride from 1200° to 1600°C," *J. Am. Ceram. Soc.*, **81** [4] 945–50 (1998).

[26]E. J. Opila, "Variation of the Oxidation Rate of Silicon Carbide with Water-Vapor Pressure," *J. Am. Ceram. Soc.*, **82** [3] 625–36 (1999).

[27]B. E. Deal and A. S. Grove, "General Relationship for Thermal Oxidation of Silicon," *J. Appl. Phys.*, **36** [12] 3770–78 (1965).

[28]E. J. Opila, J. L. Smialek, R. C. Robinson, D. S. Fox, and N. S. Jacobson, "SiC Recession Caused by SiO_2 Scale Volatility under Combustion Conditions: II, Thermodynamics and Gaseous-Diffusion Model," *J. Am. Ceram. Soc.*, **82** [7] 1826–34 (1999).

[29]W. M. Kays and M. E. Crawford, *Convective Heat and Mass Transfer*; p. 139. McGraw-Hill, New York, 1980.

[30]A. Hashimoto, "The Effect of H_2O Gas on Volatilities of Planet-Forming Major Elements: I. Experimental Determination of Thermodynamic Properties of Ca-, Al-, and Si-Hydroxide Gas Molecules and Its Application to the Solar Nebula," *Geochim. Cosmochim. Acta*, **56**, 511–32 (1992).

[31]O. H. Krikorian, "Thermodynamics of the Silica–Steam System"; p. 481 in *Symposium on Engineering with Nuclear Explosives*, Vol. 1 (Las Vegas, NV, Jan. 14–16, 1970), unpublished.

[32]M. D. Allendorf, C. F. Melius, P. Ho, and M. R. Zachariah, "Theoretical Study of the Thermochemistry of Molecules in the Si-O-H System," *J. Phys. Chem.*, **99** [41] 15285–93 (1995). □